Journal of Chromatography A, 1328 (2014) 7–15

Contents lists available at ScienceDirect

Journal of Chromatography A

journal homepage: www.elsevier.com/locate/chroma

Practical observations on the performance of bare silica in hydrophilic interaction compared with C18 reversed-phase liquid chromatography☆

James C. Heaton[a], Xiaoli Wang[b], William E. Barber[b], Stephan M.C. Buckenmaier[c], David V. McCalley[a,*]

[a] Centre for Research in Biosciences, University of the West of England, Frenchay, Bristol BS16 1QY, UK
[b] Agilent Technologies Inc., 2850 Centerville Road, Wilmington, DE 19808, USA
[c] Agilent Technologies, Hewlett-Packard Straße 8, 76337 Waldbronn, Germany

ARTICLE INFO

Article history:
Received 2 September 2013
Received in revised form
17 December 2013
Accepted 18 December 2013
Available online 27 December 2013

Keywords:
HILIC
Retention mechanism
Peak-parking
b-Term
c-Term

ABSTRACT

The kinetic performance of a bare silica and C18 phase prepared from the same sub-2 μm and 3.5 μm base materials were compared in the HILIC and RP mode using both charged and neutral solutes. The HILIC column was characterised using the neutral solute 5-hydroxymethyluridine, the weak base cytosine, and the strong base nortriptyline, the latter having sufficient retention also in the RP mode to allow comparison of performance. Naphthalene was also used as a simple neutral substance to evaluate the RP column alone. The retention factors of all substances were adjusted to give similar values ($k' \sim 5.5$) at their respective optimum linear velocities. Reduced van Deemter *b*-coefficients (determined by curve fitting and by the peak parking method, using a novel procedure involving switching to a dummy column) were significantly lower in HILIC for all substances compared with those found under RP conditions. Against expectation, *c*-coefficients were always lower in RP when compared with HILIC using sub-2 μm particles. While measurement of these coefficients is complicated by retention shifts caused by the influence of high pressure and by frictional heating effects, broadly similar results were obtained on larger particle (3.5 μm) phases. The mechanism of the separations was further investigated by examining the effect of buffer concentration on retention. It was concluded that HILIC can sometimes show somewhat inferior performance to RP for fast analysis at high mobile phase velocity, but clearly shows advantages when high column efficiencies, using longer columns at low flow velocity, are employed. The latter result is attributable to the lower viscosity of the mobile phase in HILIC and the reduced pressure requirement as well as the lower *b*-coefficients.

1. Introduction

Hydrophilic interaction chromatography (HILIC) has been gaining rapid acceptance for the analysis of hydrophilic/polar/charged solutes since the early work of Alpert et al. [1] in 1990. Arguably however, it was Martin and Synge [2] who first employed a HILIC-type separation, using a water-saturated bare silica column, albeit with the water-immiscible solvent chloroform as the mobile phase, to separate polar amino acids. The retention mechanism was likely to be similar in both studies. In HILIC, partitioning, hydrogen bonding and coulombic interactions are considered to promote retention, usually in acetonitrile rich (>70%, v/v) buffered eluents on polar stationary phases. The presence of a water-rich layer at the silanol interface on silica phases has been confirmed by both experiment [3,4] and via molecular dynamic simulation approaches [5,6]. It is between this layer and the bulk acetonitrile-rich mobile phase that analyte partitioning is thought to take place. However, depending on the nature of the analyte, partitioning only contributes in some measure to the overall retention mechanism. For instance, McCalley [7] determined that a large proportion of the retention for some basic solutes on bare silica was governed by ionic processes. There are now many commercially available polar bonded phases which can be used in HILIC providing the user with a plethora of method development choices. Irgum [8], Tanaka [9] and McCalley [10] and their co-workers have made progress in attempting to characterise the selectivity of these phases under various operating conditions. Unlike reversed-phase (RP), there

☆ Presented at the 39th International Symposium on High-Performance Liquid-Phase Separations and Related Techniques, Amsterdam, Netherlands, 16–20 June 2013.

* Corresponding author. Tel.: +44 1173282469; fax: +44 1173282904.
E-mail address: david.mccalley@uwe.ac.uk (D.V. McCalley).

0021-9673
http://dx.doi.org/10.1016/j.chroma.2013.12.058

remains difficulty in addressing general approaches to developing methods in HILIC, despite the many advantages it possesses, which is a consequence of the ill-defined separation mechanism. In addition to the enhanced retention of polar compounds, there are several distinct advantages of HILIC over RP. These include the volatility of ACN-rich mobile phases (ease of coupling and better sensitivity with mass spectrometry [11]), low operating pressures to achieve a given linear velocity [12], and different retention selectivity compared with RP [13], offering for example the potential for two-dimensional separations. Superior peak shapes may also be obtained for some compounds in HILIC compared with RP [14,15].

Despite these numerous studies, relatively little work has been published concerning the kinetic performance of HILIC compared with RP. Simple van Deemter plots show that sometimes, superior mass transfer is obtained in HILIC for basic compounds, due to the lower viscosity of the mobile phases used and resultant enhanced solute diffusivity, and that also longer columns were applicable generating high numbers of theoretical plates in a reasonable analysis time [12]. However, reduced plots, which would allow a more fundamental comparison of these techniques, were not presented in that study. In the current work, a more detailed comparison of the kinetic performance of the techniques was attempted. We used a variety of test solutes which cover a breadth of physiochemical properties in order to address the practical comparison of HILIC versus RP. These substances included a hydrophilic-neutral solute (5-(hydroxymethyl)uridine), hydrophilic-weak base (cytosine), hydrophobic-strong base (nortriptyline) and a hydrophobic-neutral (naphthalene). This range of compounds was employed as HILIC is often applied to ionised as well as polar neutral species. Acids were not included in the study as they often give very poor retention on bare silica HILIC phases due to repulsion from ionised silanol groups [10]. We employed the same native base silica from the same manufacturer for both RP and HILIC in all cases so that a better comparison of the techniques could be obtained. The *b*-coefficients were derived from peak parking experiments using a novel valve system using an additional reference column to allow immediate pressurisation of the measurement column after the parking period. Bulk diffusion coefficients (D_m) were measured experimentally using the Taylor–Aris procedure [12] and compared with values obtained from estimates using the Wilke–Chang and other procedures [16]. Peak parking derived *b*-coefficients were then compared with those from simple curve fitting of plots of reduced plate height against flow. Measurements were made with matched sub 2-μm and 3.5 μm phases, in order to determine any effect of higher pressure on the measurements. Finally, the effect of buffer concentration on retention was investigated in order to inform the interpretation of the retention mechanism in these experiments.

2. Experimental

2.1. Chemicals and reagents

HPLC grade acetonitrile was purchased from Fisher Scientific (Loughborough, U.K.). Ammonium formate, formic acid, toluene, naphthalene, uracil, 5-(hydroxymethyl)uridine, cytosine and nortriptyline were all purchased from Sigma–Aldrich (Poole, U.K.). Water at 18.2 mΩ was from a Purite Onedeo purifier (Thame, UK).

2.2. Mobile phase preparation

Pre-mixed eluents were prepared by weighing the solvents, converting to the % (v/v) values shown in Table 1 by means of their density. Stock buffer solutions of 100 mM and 125 mM were prepared by dissolving the appropriate amount of ammonium formate in water and adjusting to pH 3 using formic acid.

Table 1
Preparation of mobile phases used in the peak parking and flow studies.

Analyte	Mode	% ACN	Buffer concentration (mM/L)
Cytosine	HILIC	92.7	5.24
Nortriptyline	HILIC	94.2	5.25
5-(Hydroxymethyl)uridine	HILIC	94.8	5.93
Naphthalene	RP	54.9	n/a
Nortriptyline	RP	33.4	20.3

2.3. Apparatus and methodology

All experiments were performed on a model 1290 Infinity ultra-high pressure liquid chromatograph (UHPLC, Agilent Technologies, Walbronn, Germany) operated using Chemstation software. The instrument included a binary pump, column compartment, autosampler and diode array detector (DAD). Connections were made with minimal lengths of 75 μm ID stainless steel tubing (note these are supplied with the Agilent 1290 ultra-low dispersion kit, part number 5067-5189). The columns used were Zorbax Eclipse Plus C18 and HILIC Plus (Agilent Technologies, Delaware, USA) which were kind gifts from the manufacturer. Column dimensions were 50 mm × 2.1 mm ID in all cases using nominally 1.8, 3.5 or 5 μm packings where specified. The actual mean particle size of the 1.8 μm material in the columns used was 2.0 μm as measured by the manufacturer. This value was used in all calculations, although the nominal particle size of the material is referred to throughout. The actual particle size of the 3.5 μm material was confirmed as 3.5 μm, as measured by the manufacturer. Columns were maintained at 30 °C in the column compartment. The V_{ext} of the system was measured at approximately 9.5 μL. The DAD was equipped with a low dispersion flow cell of volume of 0.6 μL. Data collection rate was maintained at 160 Hz (although such a fast collection rate is not essential) using a bandwidth of 1.2 nm without a reference wavelength. Detector settings were 275 nm for cytosine, 240 nm for nortriptyline, 260 nm for 5-(hydroxymethyl)uridine and 210 nm for naphthalene. 1.0 μL injections of 10 ppm solutions dissolved in the exact mobile phase were used. van Deemter curves for 1.8 μm and 3.5 μm particles under HILIC conditions were constructed using flow rates from 0.025 to 2.0 mL/min (24 measurements). For the reversed-phase study using 1.8 μm particles, flow rates were 0.025–1.0 mL/min (22 measurements). For the reversed-phase comparison using 3.5 μm particles, flow rates were 0.025–1.5 mL/min (19 measurements) and 0.025–1.7 mL/min (21 measurements) for the nortriptyline and naphthalene curves respectively. Correction for extra-column effects at each flow rate was obtained using a zero-volume connector. However, due to the high *k* used for the construction of each van Deemter curve, these corrections were negligible. Cox plot analysis [17] (*k* versus 1/[M+]) for HILIC was performed at a flow rate of 0.4 mL/min and 0.3 mL/min for RP. Peak parking experiments were performed (0.4 mL/min flow) using a 6-port, 2-position dual column switching valve, which allowed the measurement column to be arrested under pressure while an identical dummy column of the same particle size and dimensions was used in place during switching times. The arrested elution times used were 0, 2, 5, 10, 20, 30 and 60 min. All measurements were performed in duplicate and averaged. For data in Fig. 1, single measurements were taken with increasing flow and the duplicate of the data point with decreasing flow to ensure no column deterioration had occurred. Symmetrical peaks were obtained in all experiments and peak widths were determined at half-height except where stated. Experimental diffusion coefficients were measured using the open tubular Taylor–Aris

Table 2
Non-reduced van Deemter coefficients from curve fitting.

Analyte	Mode	A ($\times 10^{-4}$ cm)	B ($\times 10^{-5}$ cm^2/s)	C (ms)	u_{opt} (cm/s)	H_{min} ($\times 10^{-4}$ cm)	N_{max}
d_p = 1.8 μm							
Cytosine	HILIC	2.2	3.7	0.37	0.32	4.7	10,700
5-(OH methyl)uridine	HILIC	1.9	3.2	0.61	0.23	4.7	10,300
Nortriptyline	HILIC	2.3	4.2	0.34	0.35	4.9	10,700
Nortriptyline	RP	2.5	2.8	0.47	0.24	4.8	10,400
Naphthalene	RP	2.0	8.4	0.18	0.69	4.3	11,500
d_p = 3.5 μm							
Cytosine	HILIC	4.5	3.8	0.98	0.20	8.3	6050
5-(OH methyl)uridine	HILIC	4.7	2.9	1.42	0.14	8.4	5990
Nortriptyline	HILIC	4.6	4.4	0.82	0.23	8.3	5950
Nortriptyline	RP	4.5	2.9	1.17	0.16	8.0	6270
Naphthalene	RP	3.5	8.7	0.54	0.40	7.9	6310

method using a flow rate of 0.1 mL/min at 30 °C [12]. The internal diameter and length of the PEEK tubing used was 0.05277 cm and 1500 cm, and the coil diameter was 22 cm.

3. Results and discussion

3.1. Simple van Deemter plots

In both HILIC and RP, the mobile phase strength was adjusted to give similar k' (~5.5) near their respective optimum linear velocities in order to minimise the corrections for extra-column bandspreading. These corrections were only of the order of a few %. The data was fitted to the van Deemter equation:

$$H = A + \frac{B}{u} + Cu \quad (1)$$

where H is the height equivalent to a theoretical plate, u is the linear velocity, and A, B and C are constants that can be derived from curve fitting of H versus u data. Throughout this work we refer to non-reduced coefficients in upper case, while reduced coefficients are in lower case. We compared pairs of both 1.8 μm and 3.5 μm particle packed columns. Fig. 1(a) and (c) (plots of H versus u) show the expected smaller plate heights for the smaller particle 1.8 μm HILIC and reversed-phase columns. We used a slightly higher buffer concentration for 5-(hydroxymethyluridine) in HILIC in order to maintain k at 5.5 without using less than 5% water in the mobile phase, which is a common lower limit employed. Note the retention of this solute increases with increasing buffer concentration (see below). We also used higher buffer concentrations (~20 mM) for the nortriptyline reversed-phase work so as to minimise overloading effects on the peak shape, which may be apparent even at very low sample concentrations. For this reason we did not generally employ the statistical moments approach for calculating peak profiles due to the low S/N (<100) values encountered, which can undermine the precision and accuracy of such measurements. The USP tailing factors (5% of peak height) for nortriptyline on the 1.8 μm and 3.5 μm phases were good (worst values 1.2 and 1.1 respectively), measured at their respective optimum linear velocities. Indeed Fig. 1(e) and (f) demonstrate that for these symmetric peaks, little difference was shown in the curves for nortriptyline in HILIC or naphthalene in RP when the plate height was calculated by the half-height, 5 sigma (4.4% peak height) or statistical moments method (data is shown for the smaller particle columns). Results would be expected to differ more substantially in the case of asymmetric solute peaks.

Table 2 summarises the van Deemter A, B and C coefficients for the two evaluated particle sizes. Very similar results were obtained on both the 1.8 μm and 3.5 μm columns. It can be seen on both that the B-coefficient for nortriptyline (RP) is smaller than that for the same solute under HILIC conditions. Furthermore, the C-coefficient for nortriptyline (RP) is larger than that for the same solute under HILIC conditions. These findings agree with previous results for nortriptyline [12] and are in line with expectation concerning HILIC versus RP. Table 3 shows that the experimentally measured bulk diffusion coefficient (D_m) of nortriptyline is considerably greater (more than twice) in the HILIC eluent (94.2% ACN) than that used for RP (33.4%), which as expected leads to greater axial diffusion (increased B-coefficient) but improved mass transfer (reduced C-coefficient) in HILIC. Nevertheless, whereas naphthalene (RP), 5-(hydroxymethyluridine (HILIC) and nortriptyline (HILIC) have very similar D_m in their respective mobile phases, the B-coefficient for naphthalene was considerably larger, and the C-coefficient smaller than for both the HILIC solutes. This result is unexpected, and suggests that other factors than the increased bulk diffusivity in HILIC mobile phases are involved.

It is possible that frictional heating effects might contribute to the C-coefficients at high flow rate. HILIC mobile phases have lower thermal conductivity which could contribute to radial temperature gradients. However, the low viscosity of HILIC mobile phase and consequent lower operating pressures at the same linear velocity leads to less power generation and thus may even out the effects [18]. Similar results were shown for both particle size columns, which may indicate indeed that frictional heating (which should be considerably worse for the 1.8 μm columns) had not grossly affected the results.

3.2. Determination of b-coefficients using the arrested elution method

In an attempt to interpret further the initial observations we measured the (reduced) b-coefficient using the arrested elution method [19,20]. Briefly, this procedure entails measuring the effective diffusion through the packed bed (D_{eff}) by stopping the eluent flow once the solute band has migrated about half way down the column. The flow is then resumed after a set period of time (in which diffusion of the solute takes place) and the band is eluted out of the column to the detector. The peak spatial variance is related to the parking time (t_{park}) through the relationship:

$$\sigma_x^2 = 2D_{eff} \cdot t_{park} \quad (2)$$

The equation can be written in terms of temporal variance as:

$$D_{eff} = \sigma_t^2 \cdot u_R^2 / 2t_{park} \quad (3)$$

where u_R is the retained peak velocity L/t_R and t_R is the time needed to pass through the column with length L without stopping the flow. D_{eff} can then be determined from a plot of σ_t^2 against parking time. Knowledge of the analyte diffusion coefficient in the bulk mobile phase (D_m) then allows for accurate calculation of the reduced b-coefficient from Eq. (4) [19].

$$b = 2\frac{D_{eff}}{D_m}(1 + k') \quad (4)$$

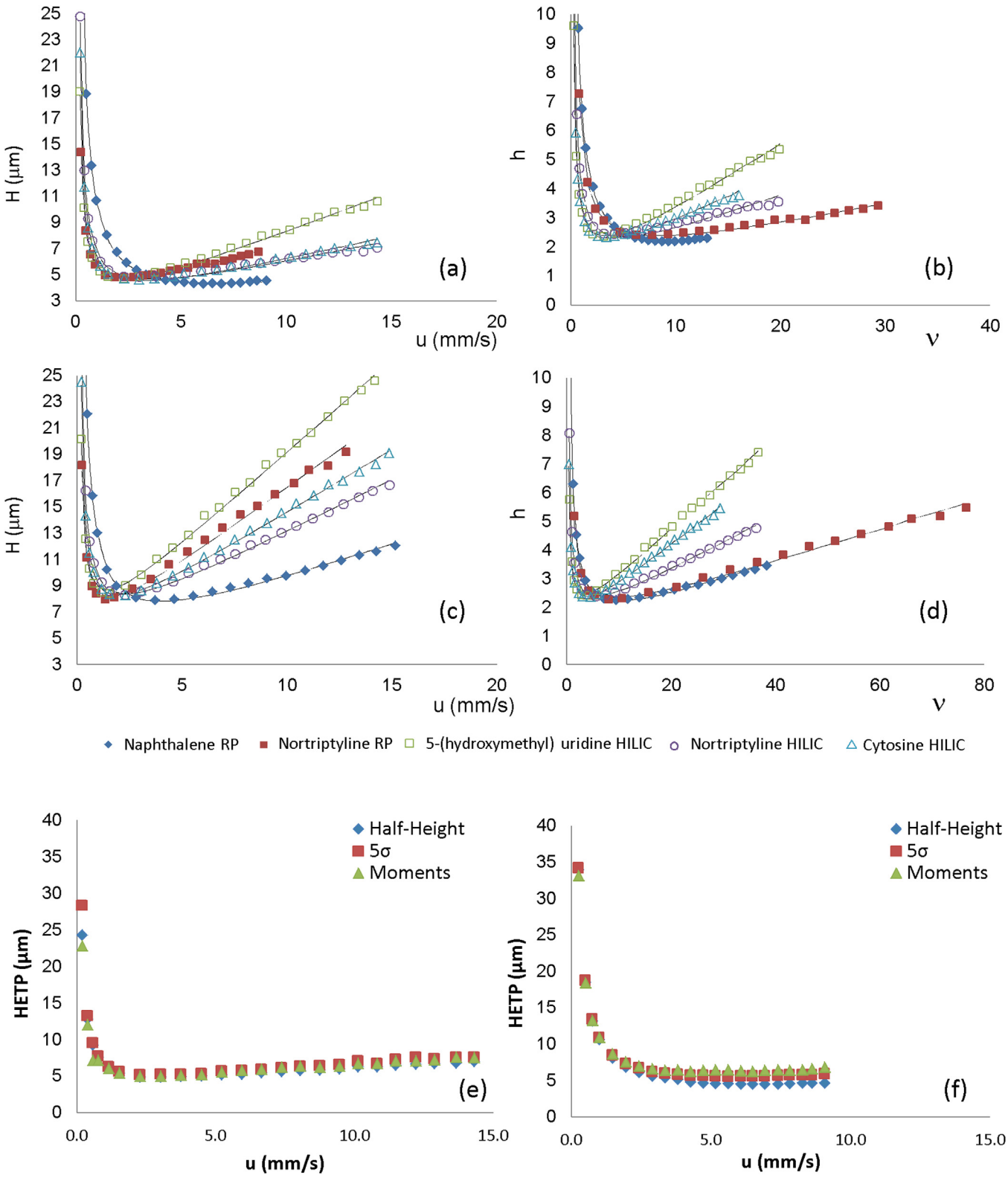

Fig. 1. Non-reduced and reduced van Deemter plots for 1.8 µm columns (a) and (b) and for 3.5 µm columns (c) and (d) respectively, using the half height method to determine plate height. Non-reduced plots for nortriptyline in HILIC (e) and naphthalene in RP mode (f) comparing the half height, 5-sigma and statistical moments method for determination of plate height. The k' for each analyte near the optimum flow velocity was around 5.5. Mobile phase as shown in Table 1. Some data points taken at lower values of u and ν are omitted to improve the clarity of figures a–d.

Carr [16] showed that correlations derived from empirical equations for determination of D_m (such as the Wilke–Chang equation) broke down in acetonitrile rich mobile phases. We therefore determined diffusion coefficients experimentally, checking our values using the value of thiourea in pure water as a reference point ($T = 25\,^{\circ}C$, $D_m = 1.33 \times 10^{-5}\,cm^2/s$ [21,22]). Table 3 confirms that very poor correlation exists between the Scheibel, Wilke–Chang and Li–Carr derived values and those determined

Table 3
Comparison of calculated versus experimental diffusion coefficients. Solvent viscosity was determined according to Ref. [43].

$T = 30\,^{\circ}C$							
Solute	% ACN	η (cP)	Calculated			Experimental	
			D_m (Scheibel)	D_m (Wilke–Chang)	D_m (Li–Carr)	D_m (Taylor–Aris)	% RSD ($n = 3$)
Cytosine	92.7	0.3968	3.29E−05	3.02E−05	3.33E−05	1.77E−05	0.40
Nortriptyline	94.2	0.3823	1.50E−05	1.49E−05	1.75E−05	1.43E−05	0.43
Nortriptyline	33.4	0.7892	6.42E−06	7.49E−06	6.07E−06	5.85E−06	0.56
Naphthalene	54.9	0.6818	1.14E−05	1.33E−05	1.19E−05	1.38E−05	0.18
5-(Hydroxymethyl)uridine	94.8	0.3777	1.89E−05	1.90E−05	2.25E−05	1.42E−05	0.70
Thiourea (25 °C)	0					1.32E−05	0.92
D_m values in cm^2/s							

Table 4
Effective diffusion data and comparison of reduced van Deemter coefficients.

Analyte	Mode	D_{eff} (cm^2/s)	D_{eff}/D_m	b (Peak Parking)	b[a] (Linearisation)	b (Curve Fitting)	c (Curve Fitting)	ν_{opt}	h_{min}
$d_p = 1.8\,\mu m$									
Cytosine	HILIC	2.58E−06	0.15	2.11	2.12	2.10	0.17	3.6	2.4
5-(OH methyl)uridine	HILIC	1.93E−06	0.14	1.94	2.27	2.26	0.22	3.2	2.4
Nortriptyline	HILIC	3.09E−06	0.22	3.06	3.04	2.94	0.12	4.9	2.5
Nortriptyline	RP	1.93E−06	0.33	4.97	4.67	4.74	0.07	8.2	2.4
Naphthalene	RP	5.26E−06	0.38	5.73	6.00	6.06	0.06	9.8	2.2
$d_p = 3.5\,\mu m$									
Cytosine	HILIC	3.01E−06	0.17	2.33	2.06	2.12	0.14	3.9	2.4
5-(OH methyl)uridine	HILIC	2.10E−06	0.15	2.21	1.92	2.01	0.17	3.5	2.4
Nortriptyline	HILIC	3.61E−06	0.25	3.35	3.06	3.08	0.10	5.7	2.4
Nortriptyline	RP	2.15E−06	0.37	5.46	4.91	4.99	0.06	9.4	2.3
Naphthalene	RP	6.12E−06	0.44	6.47	6.28	6.31	0.06	10.1	2.3

[a] Linearisation method (intercept of h versus $1/\nu$ using $n = 5$ data points, $r^2 > 0.99$ in all cases).

experimentally for some solutes under HILIC conditions. For example, a very large difference was found between the Wilke–Chang derived (3.02E−05 cm^2/s) and the experimentally determined (1.77E−05 cm^2/s) values for cytosine in 92.7% ACN. This signifies that serious errors would be encountered in determining reduced van Deemter coefficients for the b- and c-terms using calculated D_m values. Fig. 2 shows plots of peak variance versus stop time for the solute set (HILIC and RP) for both particle size columns. Excellent linearity was observed for all experiments with >0.999 r^2 values obtained for each solute. Fig. 1(b) and (d) show the van Deemter data plotted in reduced coordinates where the reduced plate height, $h = H/d_p$ and the reduced velocity $\nu = ud_p/D_m$. The HILIC and RP columns of nominally 1.8 and 3.5 μm particle size showed very similar reduced plate heights for all solutes implying they were of similar packing quality. Simplified theory indicates that plots of h versus ν for "good" columns operated under the same conditions should overlay, and be independent of d_p [23]. Typically, totally porous particle columns give values of h_{min} between 2.0 and 2.5, although this is an empirical observation; such values are indeed shown in Table 4. We deliberately measured curves for analytes at near equivalent high k, where extra-column effects only minimally influence the results.

Table 4 shows values of D_{eff} calculated from the peak parking method, and values of the reduced b-coefficient calculated from Eq. (4). Values of b- can be compared with those from curve fitting of the data in Fig. 1(b) and (d). Linearisation analysis [24] was also used to cross-check b-coefficients from curve fitting, as a sufficient number of data points were obtained in the low flow region to perform this analysis. Very good agreement is shown between the curve fitting and peak parking measurements for all solutes and conditions. It might be considered that small differences in b-coefficients measured by either method are due to shifts in k' at different flow rates in the curve fitting method (see below), because peak parking experiments involve use of the same flow rate to move the peak through and out of the column. However, there is little difference in the compared sets of values for the 1.8 and 3.5 μm columns. An advantage of our peak parking procedure

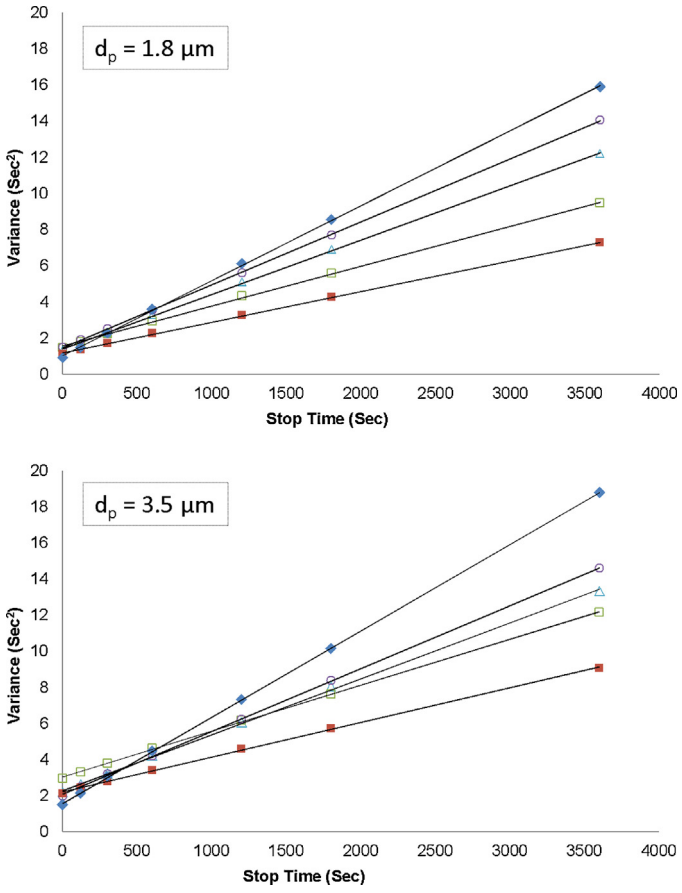

Fig. 2. Data from the arrested elution experiment for the two evaluated particles sizes. Symbols and mobile phases as in Fig. 1.

was that the arrested column was held under pressure while flow was diverted to a dummy column using a switching valve. Once the flow is resumed on the column containing the peak, minimal pressure perturbation is experienced. It could be advantageous to perform arrested elution experiments in this way as it has been argued elsewhere [25] that it is important to dampen the effect of pressure perturbations due to stopping and starting flow.

Table 4 clearly confirms the tentative conclusion of smaller *b*-coefficients in HILIC compared with RP. For example, in reduced co-ordinates, the *b*-coefficient of nortriptyline in HILIC is considerably smaller than that for the same solute in RP mode. Indeed, the *b*-coefficients for both nortriptyline and naphthalene (RP) were greater than for any of the HILIC solutes. The smaller *b*-coefficients result from the smaller values of D_{eff}/D_m for all the solutes in HILIC compared with those in RP. The observation of a smaller *b*-terms in HILIC versus RP was very recently discussed by Gritti and Guiochon [26]. Indeed, the *b*-coefficient values in our study are in agreement with these previous observations which were of the order of 2–3 for HILIC and between 5–7 for well retained solutes in RP. In RP chromatography, surface diffusion provides a considerable contribution to the *b*-term of non-polar solutes retained by a non-localised retention mechanism. The *b*-term may be made up of three distinct contributions [27]. Firstly, diffusion occurs outside the particle in the mobile phase, secondly in the mesopores of the particle and thirdly along the pore surface of the stationary phase (surface diffusion) [28]. For hydrophobic neutral substances in RP, surface diffusion is facilitated by the organic-rich layer associated with the C18 ligands. The surface diffusion effect is understood to account for a large proportion of the intra-particle diffusion character of a retained solute in RP [29]. Apparently, the mobility of analytes interacting with a solid silica surface in the HILIC mode is more restricted. It has been suggested that this implies an adsorption mechanism in HILIC (at least with bare silica columns) in which localised interactions of the solute take place with specific silanol sites of various kinds on the phase surface [30]. Additionally, although surface diffusion could also be considered to occur in HILIC, it would of necessity have to take place in a high viscosity water layer and thus would contribute little to the intra-particle diffusivity. The viscosity of pure water is 2–3 times greater than that of pure acetonitrile [31]. As solute diffusivity is inversely related to the viscosity, surface diffusion in the HILIC water layer would be expected to be considerably less than that in the surface layer of ACN associated with a C18 stationary phase. Localisation has been given as the reason for small *b*-coefficients measured in adsorption chromatography (normal phase) with bare silica columns in studies performed more than 30 years ago by Snyder and co-workers [32]. Indeed, adsorption is a component of the retention mechanism in HILIC that is likely to be encouraged on bare silica columns which have less extensive water layers [4], especially with the rather low mobile phase water concentrations used in the present experiments [3].

We have performed these studies with a single mobile phase per sample and column giving high *k*. Previous studies have shown that in RP the reduced *b*-coefficient reaches a broad maximum value at high *k*, whereas stabilisation of *b* occurs rapidly in HILIC [26]. We believe that this approach allows a more reliable comparison of the modes to be made.

While reduced plots are more useful in interpreting underlying processes, consideration of non-reduced plots remains of importance to the practitioner, as these plots demonstrate what will be observed by an experimentalist (see also kinetic plots below).

3.3. Comparison of c-coefficients

It is clear that from the reduced plots in Fig. 1 that analysis at high velocity gives rise to larger reduced plate heights in HILIC compared with RP, while *h* values at the optimum flow velocity are remarkably similar. It is possible to explain this result as being due to slower adsorption–desorption kinetics in HILIC, although there is little firm evidence in the literature to support such a hypothesis. Alternatively, Guiochon [30] has suggested that the majority of this band broadening effect is due to long range eddy dispersion. It was argued that the transverse diffusion coefficient (which is scaled to the diffusion coefficient of the analyte) is too small and the column ID too large to allow complete relaxation of the radial concentration gradient within the column. This effect would therefore be greater in reduced plots for HILIC compared with RP, due to lower surface diffusion. Gradients may originate at the column inlet due to a non-uniform sample distribution and at the column outlet due to asynchronous sample collection when standard end fittings are used [30]. It was noted that some variation in the transverse diffusion coefficients might be obtained from one average particle diameter to another, which could explain the differences in the *c*-term region of the reduced plots in Fig. 1(b) and (d). The effects would be reduced with long narrow columns, providing that the bed structure of narrow columns showed good radial homogeneity of the bed structure (which of course, is not often the case). Thus at least for columns of the same dimensions, fast analysis should be more favoured using RP chromatography.

It is not possible to make firm conclusions on this issue from our present work, as the *c*-coefficients deduced are a mixture of the contribution of mass transfer and eddy dispersion. The latter is assumed to be independent of flow in the simplified van Deemter treatment used in this study (Eq. (1)) whereas clearly it is not.

A further comparison of kinetic performance is available through kinetic plots as this method also considers the differences in viscosity between the eluents used in HILIC and RP (see below).

3.4. Effect of flow on retention

The measurement of parameters related to solute retention on small particle columns is complicated by the effects of frictional heating and pressure which both increase as flow is increased. These effects can be solute dependent. Indeed, significant changes in retention factor were observed for all analytes in both RP and HILIC modes (Fig. 3), which shows the % loss in retention going from the lowest to the highest flow used for 1.8, 3.5 and also 5 μm columns, introduced to compare effects at the lowest pressures. For all columns, the lowest flow rate used was 0.025 mL/min. The highest flow rates used for 1.8 μm particle evaluation in HILIC was 2.0 mL/min and 1.0 mL/min in RP. For the 3.5 μm column in HILIC, the maximum flow was 2.0 mL/min, whereas for RP conditions the maximum flow used was 1.5 mL/min and 1.7 mL/min for nortriptyline and naphthalene data respectively. Clearly, the effects of high flow on retention are greatest for the 1.8 μm column and least for the 5 μm column. These effects are rarely mentioned in studies of column performance as a function of flow.

Fig. 3 shows a small % loss in *k* between high and low flow for naphthalene in the RP mode which is most significant for the 1.8 μm column. Values of *k* usually decrease with increasing temperature [33] and indeed in columns of similar dimensions, temperature increases of up to 20 °C have been noted due to frictional heating [34]. Increased pressure in the absence of heating effects, however increases retention for simple aromatic compounds in RP, with greater increases shown for compounds with increasing MW. Thus anthracene (which has a higher MW than naphthalene) gave an increase in *k* of about 10% for a 500 bar pressure increase [35]. The overall change in *k* for naphthalene is a balance of these two effects, which act in opposition. Nortriptyline in RP shows overall *increases* in retention with increasing flow (Fig. 3). This result is explained by a much larger increase in *k* with pressure alone (~50% for a

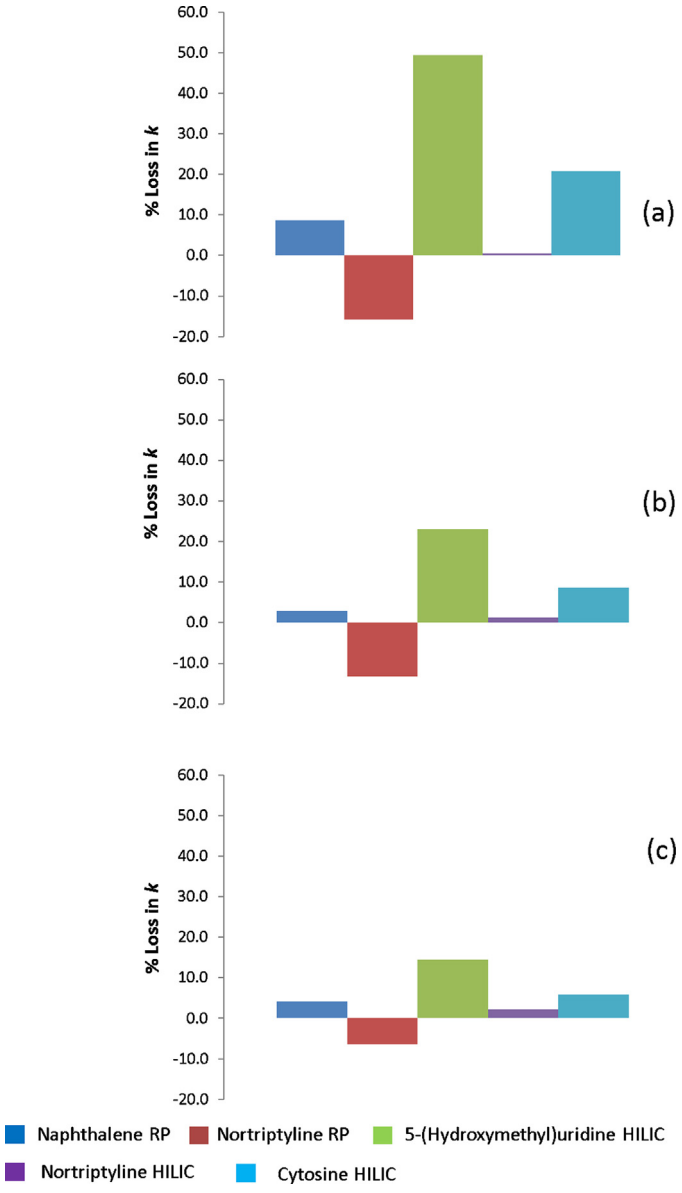

Fig. 3. Percentage loss in k between the highest and lowest flow rate used (detailed in Section 3.4) for (a) 1.8 μm, (b) 3.5 μm and (c) 5 μm particles.

500 bar pressure increase [35]) for this higher MW ionic species. Cytosine and 5-(hydroxymethyluridine) show large *decreases* in retention with increased flow. In HILIC, increased pressure alone appears to reduce k [36,37] and therefore the effects of pressure and temperature act in the same direction. For nortriptyline in the HILIC mode, increased temperature exceptionally appears to increase retention [10]. Therefore pressure and temperature effects balance out leading to the small variation in k with flow indicated in Fig. 3.

It is conceivable that the variations in k with flow shown in Fig. 3, especially for the 1.8 μm column might have affected the values of the reduced b- and c-coefficients for this column. However, results for these coefficients are similar on the larger particle 3.5 μm column, which showed much smaller variations in k with flow (see Table 4). This finding gives confidence that the coefficients deduced by curve fitting are not seriously influenced by k variation, or by the effects of frictional heating due to the mobile phase percolation through the packed bed.

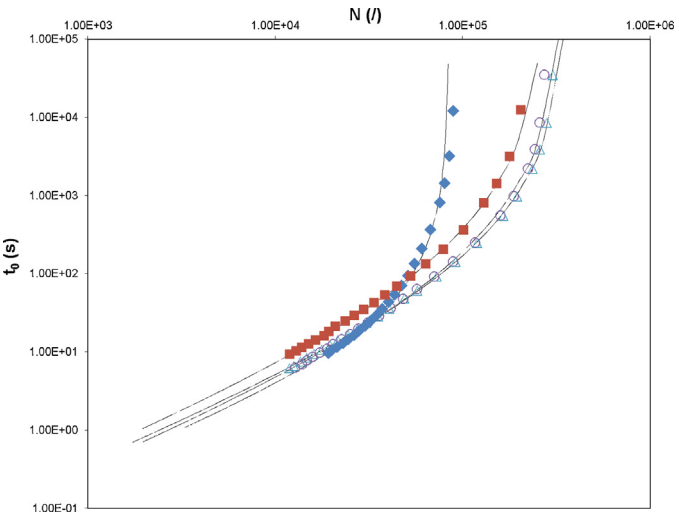

Fig. 4. Kinetic plot of t_o versus N for HILIC and reversed-phase using a pressure maximum = 1000 bar for the 1.8 μm particle packed columns. Symbols are as in Fig. 1.

3.5. Kinetic plot comparison between HILIC and RP modes

The influence of the B-term and eluent viscosity (η) on the maximum achievable kinetic performance is established by considering the following expression of Desmet et al. [38]:

$$N_{max} = \frac{\Delta P}{\eta}\left[\frac{K_v}{B}\right]_{exp} \quad (5)$$

Operating a length of column at a fixed pressure max (ΔP) with a specific bed permeability (K_v) any reduction in both the B-coefficient and viscosity would afford higher achievable maximum plate numbers. By increasing column length to afford larger plate numbers, higher pressures are required to achieve linear velocities in excess of the optimum velocity to limit the contribution of the B-term to efficiency. The moderate B-coefficients in HILIC combined with the low viscosity of the mobile phases therefore offers particular advantages in accommodating long columns for high resolution analysis. The lower mobile phase viscosity might contribute positively to fast analysis, since higher linear flow velocities can be adopted within the pressure limit of the instrument. Furthermore, for some solutes that can be analysed in either HILIC or RP mode, enhanced diffusion coefficients in HILIC should favourably promote mass transfer in fast analysis.

Fig. 4 shows the simplest kinetic plot representation of transformed van Deemter data into column dead time t_o versus efficiency N. These plots were constructed for the 1.8 μm particle packed columns only, using a pressure maximum of 1000 bar, for all the solutes except 5-(hydroxymethyl)uridine, which was omitted due to the large losses in retention (noted above) caused by the influence of flow/pressure. With respect to the naphthalene (RP) curve (diamond symbol), the impact of the larger B-term and the higher viscosity of the mobile phase is patently obvious at the right-hand side of the plot at high values of N. In order to shift the vertical asymptote of this curve towards larger plate numbers, much higher pressures would be required to deliver adequate linear velocities through the correspondingly longer columns. In contrast, it is possible to obtain in excess of 100,000 plates for nortriptyline in RP due to the smaller (non-reduced) B-term, due in part to its lower D_m value. Higher plate counts for the HILIC solutes are achievable due principally to the lower viscosity of the mobile phases. At t_o = 500 s the predicted plate counts were 76,000, 110,000, 144,000 and 154,000 for naphthalene (RP), nortriptyline (RP), nortriptyline (HILIC) and cytosine (HILIC) respectively.

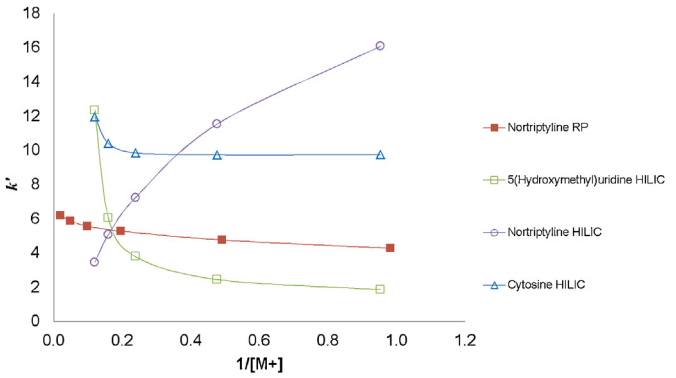

Fig. 5. (a) Plot of Log k' versus Log [M+] and (b) k' versus 1/[M+]. HILIC conditions were 94.8% ACN containing 1–8 mM overall ammonium format$^{w}_{w}$ pH 3.0 and reversed-phase was 33.4% ACN containing 1–50 mM overall ammonium format$^{w}_{w}$ pH 3.0.

However, the achievement of such plate counts entails the use of very long columns, the predicted lengths being around 60 cm for RP conditions and 80 cm for HILIC.

The curves also indicate the relative performance at short analysis times (left hand side of the plots). At t_o = 10 s the predictions were 19,000, 12,600, 17,000 and 16,800 plates for naphthalene (RP), nortriptyline (RP), nortriptyline (HILIC) and cytosine (HILIC) respectively. The predicted columns lengths for the fast analysis region were around 10 cm. The differences in the plate counts relates to those particular column lengths being operated at 1000 bar and well into the *C*-term dominated region. Recall that naphthalene in RP had a very low *C*-coefficient with little loss in efficiency observed in the high flow region (Fig. 1). In contrast, the poorer performance of nortriptyline in RP mode in the *C*-term region of the plot is due to its low mobile phase diffusion coefficient. As with any kinetic plot predictions caution must be adhered to as the initial van Deemter data were constructed using 5 cm long columns. Ruta et al. [39] pointed out that differences in the packing qualities of longer columns, or frictional heating effects, make it difficult to realise accurately in practice the predictions made for long/coupled columns.

3.6. Retention mechanism elucidation

In order to discover more about the retention mechanism in the different separation modes, particularly with regard to ionic processes, we investigated the effect of buffer strength on k'. Cox and Stout [17] investigated ionic retention using plots of k' versus 1/[M+] where [M+] is the concentration of the displacing buffer cation of the same charge as the solute. These plots should be linear for a pure cation-exchange process for basic compounds, with the line passing through the origin at infinite buffer concentration. A *y*-axis intercept of the plot allows the contribution of non-ionic processes to retention to be assessed. Fig. 5 shows the plots for HILIC (94.8% ACN containing 1–8 mM overall ammonium formate$^{w}_{w}$ pH 3.0) and reversed-phase (33.4% ACN containing 1–50 mM overall ammonium formate$^{w}_{w}$ pH 3.0). The column hold-up volume (V_m) was determined using the non-retained compound toluene in HILIC, and uracil in RP. These markers were incorporated in every injected sample, as V_m can depend on mobile phase properties such as the ionic strength [40]. Fig. 5 shows that the retention of nortriptyline in HILIC decreases substantially as the buffer concentration increases, indicating the presence of ionic retention. The curvature of the plot is similar to that found in a previous study [7], also using a bare silica stationary phase (Luna, Phenomenex). It is possible this curvature could be due to a small degree of ion pairing, which has been suggested as feasible at least with the acetate anion [41]. The curvature precludes the accurate estimation of the contribution of ion exchange to retention that would be possible with a linear plot, but extrapolation to infinite buffer concentration indicates that a very high proportion of the retention process is due to ion exchange. In contrast, nortriptyline in RP mode shows a small *increase* in retention with increasing buffer strength, indicating the absence of cation exchange under these conditions. It is possible that the presence of hydrophobic ligands reduces the acidity of silanol groups in the RP mode and thus also reduces the influence of ion exchange, as these stationary phases use the same base silica. The small increase in retention for nortriptyline with increasing buffer strength might again be attributed to ion-pair effects, although these are likely to be much smaller than in HILIC due to the lower concentration of acetonitrile in the RP mobile phase. Alternatively, it is possible that some positively charged groups exist on the RP surface that are introduced in the bonding process [42]. The repulsive effect of such groups would be moderated with increasing buffer concentration. The strong component of ionic retention of nortriptyline in HILIC could well influence its smaller value of the *b*-coefficient found in this mode compared with RP (see Table 4 and discussion in 3.2), due to reduction of surface diffusion effects. The weak base cytosine does not appear to be charged under the HILIC conditions used, as its retention increases with increasing buffer strength (Fig. 5(b)). Increase in retention with increasing buffer strength is also shown for the neutral 5-(hydroxymethyl)uridine. It is possible that the increased buffer strength increases the contribution of the partition process to retention for these compounds, by increasing the thickness of the water layer on the silica surface. Clearly, the effects of buffer concentration have only been studied at the single organic solvent concentration used for each solute in the kinetic studies. It is quite possible that the balance of the various contributing mechanisms changes with % organic, and a more comprehensive series of experiments would be necessary to examine this question further.

In summary, the nature of the interactions in both chromatographic modes is complex. It should certainly be considered that these interactions influence the mobility of analytes in the adsorbed state.

4. Conclusions

Significant differences in both the reduced and non-reduced axial diffusion behaviour of solutes in the RP and HILIC modes were observed on columns made from the same silica. These differences were evaluated using curve fitting of the van Deemter equation to data of plate height versus flow and by peak parking experiments. A novel method was employed using switching flow to a dummy column during the parking step. Simple non-reduced plots for the same basic compound (e.g. nortriptyline) in either mode indicated that *B*-coefficients were larger in HILIC than RP, and *C*-coefficients were smaller. Thus the practitioner will observe lower efficiency at low flow rate but higher efficiency at high flow rate in HILIC compared with RP for similar basic compounds. These results are as expected, and attributable merely to the much higher solute diffusivity of such compounds in the low viscosity, high ACN concentration mobile phases used for them in HILIC compared with RP.

However, comparison of both basic and neutral solutes in reduced coordinates confirmed that the *b*-coefficients (determined by peak parking, and by curve fitting) for all solutes studied in the HILIC mode were considerably smaller than for those studied in the RP mode. An explanation of these results, based on the work of Guiochon and others, is that in RP, surface diffusion can take place due to the non-localised retention mechanism, facilitated by the layer of acetonitrile on the surface of the stationary

phase, increasing the *b*-coefficient. In contrast, in HILIC, localised adsorption (or ionic retention) may contribute significantly to the retention mechanism, at least for bare silica columns using mobile phases of relatively low water content. Surface diffusion in the layer of water on the surface of HILIC columns also seems much less likely. The reduced *c*-coefficients were always higher in HILIC than RP. This could be due to slower adsorption–desorption kinetics in HILIC, but further experiments are necessary to establish whether this, or other interpretations of the increased values, are more likely [30].

The nature of the mechanism in HILIC is ill-defined as was shown by the effect of varying buffer concentration on retention. Ionic retention of cations appears to play a much greater role in HILIC than RP. However, the retention mechanism may be significantly different on bonded phase HILIC columns compared with the bare silica columns used in this study. Practitioners should be wary of retention factor shifts at high flow rate that are particularly apparent for some solutes in HILIC, where for other solutes, decrease in retention both with increased pressure and with increased temperature act in the same direction. Nevertheless, comparable results were obtained in the present study for both sub-2 μm and larger particle stationary phases, showing that the deductions were not grossly affected.

Kinetic plot analysis shows HILIC can give improved performance over RP when high efficiencies are required, using long columns at low flow rates. This improvement results from the low viscosity of typical HILIC mobile phases, allowing the use of longer columns, together with the effect of lower *B*-coefficients than expected. For fast analysis on short columns, the advantage of low mobile phase viscosity in HILIC is opposed by higher *C*-coefficients than might be expected.

Acknowledgment

This work was supported by the United Kingdom Engineering and Physical Sciences Research Council [grant number EP/J016578/1]. The authors thank Anne Mack at Agilent Technologies for exploratory work on comparing HILIC and RP.

References

[1] A.J. Alpert, J. Chromatogr. 499 (1990) 177.
[2] A.J. Martin, R.L. Synge, Biochem. J. 35 (1941) 1358.
[3] D.V. McCalley, U.D. Neue, J. Chromatogr. A 1192 (2008) 225.
[4] N.P. Dinh, T. Jonsson, K. Irgum, J. Chromatogr. A 1320 (2013) 33.
[5] S.M. Melnikov, A. Höltzel, A. Seidel-Morgenstern, U. Tallarek, Anal. Chem. 83 (2011) 2569.
[6] S.M. Melnikov, A. Höltzel, A. Seidel-Morgenstern, U. Tallarek, Angew. Chem. (Int.) 51 (2012) 6251.
[7] D.V. McCalley, J. Chromatogr. A 1217 (2010) 3408.
[8] N.P. Dinh, T. Jonsson, K. Irgum, J. Chromatogr. A 1218 (2011) 5880.
[9] Y. Kawachi, T. Ikegami, H. Takubo, Y. Ikegami, M. Miyamoto, N. Tanaka, J. Chromatogr. A 1218 (2011) 5903.
[10] A. Kumar, J.C. Heaton, D.V. McCalley, J. Chromatogr. A 1276 (2013) 33.
[11] N. Gray, J. Heaton, A. Musenga, D.A. Cowan, R.S. Plumb, N.W. Smith, J. Chromatogr. A 1289 (2013) 37.
[12] D.V. McCalley, J. Chromatogr. A 1193 (2008) 85.
[13] J. Ruta, S. Rudaz, D.V. McCalley, J.-L. Veuthey, D. Guillarme, J. Chromatogr. A 1217 (2010) 8230.
[14] D.V. McCalley, J. Chromatogr. A 1171 (2007) 46.
[15] J. Heaton, N. Gray, D.A. Cowan, R.S. Plumb, C. Legido-Quigley, N.W. Smith, J. Chromatogr. A 1228 (2012) 329.
[16] J. Li, P.W. Carr, Anal. Chem. 69 (1997) 2530.
[17] G.B. Cox, R.W. Stout, J. Chromatogr. 384 (1987) 315.
[18] D.V. McCalley, J. Chromatogr. A 1218 (2011) 2887.
[19] J.H. Knox, H.P. Scott, J. Chromatogr. 282 (1983) 297.
[20] A. Liekens, J. Denayer, G. Desmet, J. Chromatogr. A 1218 (2011) 4406.
[21] D.B. Ludlum, R.C. Warner, H.W. Smith, J. Phys. Chem. 66 (1962) 1540.
[22] P.J. Dunlop, C.N. Pepela, B.J. Steel, J. Am. Chem. Soc. 92 (1970) 6743.
[23] L.R. Snyder, J.J. Kirkland, Introduction to Modern Liquid Chromatography, 2nd ed., Wiley, New Jersey, 1979.
[24] J. Li, P.W. Carr, Anal. Chem. 69 (1997) 2193.
[25] F. Gritti, G. Guiochon, J. Chromatogr. A 1218 (2011) 896.
[26] F. Gritti, G. Guiochon, J. Chromatogr. A 1297 (2013) 85.
[27] G. Desmet, K. Broeckhoven, J. De Smet, S. Deridder, G.V. Baron, P. Gzil, J. Chromatogr. A 1188 (2008) 171.
[28] K. Miyabe, G. Guiochon, J. Chromatogr. A 1217 (2010) 1713.
[29] F. Gritti, G. Guiochon, J. Chromatogr. A 1128 (2006) 45.
[30] F. Gritti, G. Guiochon, J. Chromatogr. A 1302 (2013) 55.
[31] H. Colin, J.C. Diez-Masa, G. Guiochon, T. Czajkowska, I. Miedziak, J. Chromatogr. 167 (1978) 41.
[32] R.W. Stout, J.J. DeStefano, L.R. Snyder, J. Chromatogr. 282 (1983) 263.
[33] L.R. Snyder, J.J. Kirkand, J.W. Dolan, Introduction to Modern Liquid Chromatography, 3rd ed., Wiley, New Jersey, 2010.
[34] K. Kaczmarski, J. Kostka, W. Zapala, G. Guiochon, J. Chromatogr. A 1216 (2009) 6575.
[35] M.M. Fallas, U.D. Neue, M.R. Hadley, D.V. McCalley, J. Chromatogr. A 1209 (2008) 195.
[36] M.M. Fallas, U.D. Neue, M.R. Hadley, D.V. McCalley, J. Chromatogr. A 1217 (2010) 276.
[37] U.D. Neue, C.J. Hudalla, P.C. Iraneta, J. Sep. Sci. 33 (2010) 838.
[38] G. Desmet, D. Clicq, P. Gzil, Anal. Chem. 77 (2005) 4058.
[39] J. Ruta, D. Zurlino, C. Grivel, S. Heinisch, J.-L. Veuthey, D. Guillarme, J. Chromatogr. A 1228 (2012) 221.
[40] G. Greco, S. Grosse, T. Letzel, J. Chromatogr. A 1235 (2012) 60.
[41] D.H. Marchand, P.W. Carr, D.V. McCalley, U.D. Neue, J.W. Dolan, L.R. Snyder, J. Chromatogr. A 1218 (2011) 7110.
[42] D.V. McCalley, Anal. Chem. 78 (2006) 2532.
[43] H. Chen, C. Horvath, Anal. Meth. Instrum. 1 (1993) 213.